ChemComm

Check for updates

Polar organic cages for efficiently separating azeotropic mixtures†

Lukman O. Alimi, Xin Liu, [ID] Gengwu Zhang, Basem Moosa [ID] and Niveen M. Khashab [ID] *

Dihydroxy-based polar organic cages (DIHO-cages) are reported to selectively separate toluene with 99.5% purity from an equimolar toluene/pyridine mixture, resulting in subsequent superior purification of pyridine. The efficient separation and purification, enhanced by strong and multiple host/guest C−H···O interactions between the cage and toluene, showcases DIHO-cages as a suitable candidate for the remarkable separation of such azeotropes on an industrial scale.

One of the representative polar organic solvents that have been identified as "preferred" or "usable" industrial solvents is pyridine.[1] Pyridine with a boiling point of 115.3 °C is an important catalyst and solvent that is widely used in agrochemical, pharmaceutical and petrochemical industries.[1] Most importantly, the demand for pyridine globally is mostly driven by its increased pharmaceutical use and use as a denaturant in antifreeze mixtures.[2] On the other hand, toluene is heavily used to manufacture pesticides, coatings, synthetic resins, explosives, polyesters and benzoic acid.[1] Both toluene and pyridine are important industrial chemicals but pyridine often forms a minimum boiling binary azeotrope with toluene (boiling point 110.0 °C; pyridine/toluene 23 : 77, molar basis) during production, making separation of toluene from pyridine a difficult task; therefore, their purification has remained a great challenge.[3,4] Although several methods have been used with great success to separate and purify azeotropic mixtures, including azeotropic distillation,[5] pressure-swing distillation,[6,7] and extractive distillation[8] as well as other techniques, these methods have been bedevilled by high operating costs, high energy consumption and technical complexities.[9] So, the need for better and cost-effective methods is urgent and necessary. Some new separation strategies

Smart Hybrid Materials Laboratory (SHMs), Physical Science and Engineering, King Abdullah University of Science and Technology (KAUST), Thuwal, 23955-6900, Saudi Arabia. E-mail: niveen.khashab@kaust.edu.sa

that have emerged recently involve the use of the differences in the noncovalent interactions that exist between guests and crystalline nonporous adsorptive materials.[10–17] A few examples of these crystalline nonporous adsorptive materials have been reportedly used for separation of minimum-boiling binary azeotrope mixtures involving polar compounds such as pyridine.[18–20] The report by Chi and coworkers described the use of a new cavity-extended version of calix[4]pyrrole (C4P) that forms nonporous adaptive crystals for the effective separation of polar compounds from pyridine/toluene and 1,4-dioxane/water azeotrope mixtures.[18] In another study by Huang and coworkers, nonporous adaptive crystals of cucurbit[6]uril (Q[6]) could, by forming a host/guest complex, separate pyridine from a toluene/pyridine mixture with 100% purity.[19] Also, Isaacs and coworkers reported the separation of pyridine from azeotrope mixtures of toluene, benzene and pyridine with more than 99.9% purity even in a system with low pyridine content by using double-cavity nor-seco-cucurbit[10]uril (ns-Q[10]).[20a] Most recently, Li and coworkers reported the use of macrocycle cocrystals for efficient removal of pyridine from an equimolar toluene/pyridine mixture with 99.2% purity.[20b] Common to all these examples is that the separation occurs using the intrinsic cavity[18,19,20a] of specific dimensions as revealed by the crystal structures of their respective macrocycles and that these cavities could only capture the smaller-sized pyridine.

As part of the ongoing work in our group in the quest for organic cages showing excellent separation performances/applications, we have prepared and deployed a polar **DIHO-cage** endowed with hydrogen-bond-donor hydroxyl (–OH) groups and the possibility of forming extrinsic pores in their crystal packing that can accommodate any of these mixtures for efficient separation, in contrast to the case for macrocycles with fixed/pre-sized cavities. We have also recently established that a pre-sized or fixed cavity dimension is not a prerequisite for excellent separation, most especially when larger guest molecules are involved.[21] Herein, we utilized the polar organic **DIHO-cage** as adsorptive materials to separate an equimolar mixture of toluene/pyridine. Surprisingly, **DIHO-cage** can capture and separate **Tol** from an equimolar **Tol/Py** mixture with

Scheme 1 Schematic representation of **DIHO-cage** as an adsorptive material for separation of toluene from pyridine in an equimolar mixture.

Fig. 1 PXRD patterns showing the adsorption of **Tol** and **Py** by the **DIHO-cage** after 24 h exposure.

99.5% purity unlike most of the reported cases where pyridine is captured[18–20] instead of toluene (Scheme 1). To the best of our knowledge this is the first example of using a polar organic cage for efficient selective separation of **Tol** and subsequent purification of the polar compound **Py** from a **Tol/Py** binary mixture.

DIHO-cage was synthesized, with a good 70% yield, by carrying out a simple, cost-effective and one-step condensation reaction of 2,5-dihydoxyterephtahaldehyde with flexible tris(2-aminoethyl)amine (TREN) in acetonitrile (Scheme S1, ESI†).[22] Proton, ^{13}C NMR and mass spectra confirmed the successful synthesis of **DIHO-cage** (Fig. S1 and S2, ESI†). We chose **DIHO-cage** as our adsorbent as mentioned earlier because of its polar nature that would not only promote host/guest hydrogen bonding but also boost crystallinity.[23] Two different types of suitable single crystals of **DIHO-cage**, denoted as **DIHO-cage@DCM** and **DIHO-cage@CHCl₃**, were obtained by diffusing acetonitrile into, respectively, DCM and chloroform solutions of **DIHO-cage** (Fig. S3 and Table S1, ESI†). **DIHO-cage@DCM** was observed to crystallize in the monoclinic system, specifically with the space group $P2_1/c$, and **DIHO-cage@CHCl₃** also crystallized in monoclinic system, but with the space group $C2/c$. Analysis of the crystal structures of **DIHO-cage** with DCM and chloroform revealed a high propensity for **DIHO-cage** to form complexes with most organic solvents utilizing the extrinsic pores in the crystal packing of the cage, like some other reported (2+3) organic cages (Fig. S1, ESI†).[22,24–27] In fact, inspection of the crystal structure of **DIHO-cage@DCM** showed two guest molecules of DCM with one molecule of the cage in the asymmetric unit, while inspection of the **DIHO-cage@CHCl₃** crystal structure showed one molecule of the cage with one molecule of chloroform in the asymmetric unit (Fig. S3, ESI†).

Thermogravimetric analysis (TGA) of the as-synthesized **DIHO-cage** showed no appreciable weight loss as the temperature was increased up to 300 °C, indicating that it had no solvent left after being synthesized. Despite this lack of residual solvent in the as-synthesized cage, we decided to activate it at 40 °C for 2 h to ensure that it remained empty before use for all the subsequent experiments (Fig. S4, ESI†). Powder X-ray diffraction (PXRD) confirmed the bulk purity of the as-synthesized **DIHO-cage**. The PXRD pattern of the activated **DIHO-cage** confirmed that its crystallinity was retained after it was subjected to the desolvation procedure (Fig. S5, ESI†). The Brunauer–Emmett–Teller (BET) surface area of the
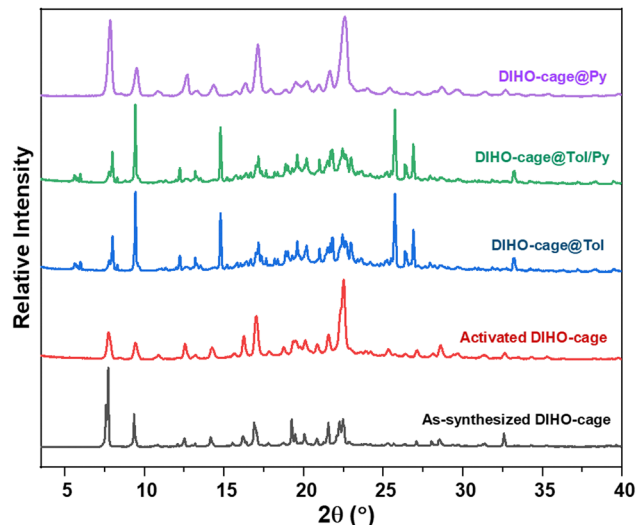
activated **DIHO-cage** was determined to be 14 m² g⁻¹ according to the N₂ gas sorption isotherm at 77 K, indicative of **DIHO-cage** being non-porous (Fig. S6, ESI†). The adsorption efficiency of the activated **DIHO-cage** in the presence of a mixture of pyridine and toluene was then tested by performing solid–vapour adsorption experiments. Notably, PXRD and ^{1}H-NMR results for single-component and 1:1 (v/v) binary mixture experiments indicted that **DIHO-cage** may be selective for toluene over pyridine (Fig. 1 and Fig. S7, ESI†).

The adsorption performance of **DIHO-cage** was further investigated using different ratios of **Tol** to **Py** (1:3 and 3:1 (v/v)) to replicate the ideal industrial situation and further understand the influence of these ratios on the **DIHO-cage** performance. The results of ^{1}H-NMR and gas chromatographic analyses of **DIHO-cage** samples exposed to these different ratios of toluene to pyridine confirmed a selective adsorption of toluene over pyridine with relatively high purity levels of 97.4% and 99.9% for, respectively, 1:3 and 3:1 (v/v) Tol/Py mixtures after one adsorption process (Fig. S8 and S9, ESI†). To investigate the dynamics of the adsorption process, we carried out time-dependent solid-vapour sorption experiments. It took **DIHO-cage** about 10 h to accommodate on average *ca.* 1.0 mole of **Tol** per cage, with an adsorption capacity of 134.9 mg g⁻¹ (Fig. S10, ESI†). To better understand the mechanism of the selective adsorption of **Tol** over **Py**, first single crystals of **DIHO-cage@Tol** were grown by effecting vapour diffusion of MeCN into a toluene/DCM solution of **DIHO-cage** at room temperature (Table S1, ESI†). Single crystals of **DIHO-cage@Py** were also obtained using the same approach with **Py**. Inspection of the crystal structure of **DIHO-cage@Tol** showed a 1:1 ratio of **DIHO-cage** to **Tol** (Fig. S11, ESI†).

In the crystal structure, the **Tol** guest molecules were situated, as expected, in the extrinsic cavity generated by the crystal packing (Fig. 2 and Fig. S12, ESI†). Inspection of the crystal packing of **DIHO-cage@Tol** showed **Tol** molecules situated

Fig. 2 Perspective view showing **Tol** guest molecules (pink) in the crystal packing of **DIHO-cage@Tol**.

between the two layers and forming a continuous channel when viewed along *b*-axis (Fig. S12, ESI†). Inspection of the crystal structure also showed multiple C–H⋯O host/guest intermolecular interactions, including those with lengths of 3.434 Å, 3.497 Å and 3.756 Å occurring between some of the protons on the **Tol** molecule and the oxygen atom of the –OH group on the cage molecule (Fig. 3 and Fig. S13 and Table S2, ESI†). The crystal packing also showed other noncovalent intermolecular interactions (*e.g.*, C–H⋯π = 3.703 Å, *etc.*) between some of the protons of the cage and the centroid of the aromatic ring of the **Tol** guest (Fig. 3).

Some host/host intermolecular interactions between two neighbouring cages also formed (Fig. S14 and Table S3, ESI†). Unlike the case for **DIHO-cage@Tol**, no **Py** guest molecule was found in the crystal structure of **DIHO-cage@Py**. The ability of **DIHO-cage** to form a complex with only **Tol** suggested its bias to favour the uptake of **Tol** from a **Tol/Py** mixture.

Furthermore, in all of the crystal structures available, very strong O–H⋯N intramolecular hydrogen bonding interactions formed within the cage (Fig. S15, ESI†). These strong intramolecular interactions, apart from preventing the aromatic groups from rotating, would appear to also outcompete any possibly formed intermolecular interactions, rendering the hydrogen atom on the –OH groups unavailable as an H-bond donor for intermolecular host–guest hydrogen bonding

interactions, perhaps explaining why **Py** (H-bond acceptor) was not observed to have been captured by **DIHO-cage**.[28] Having established the ability of the **Tol** guest molecule to interact with **DIHO-cage**, it is important to mention that the size and/or shape of **Tol** could have also contributed to this selective uptake. **DIHO-cage** using its extrinsic cavity for the uptake implies no limitation on the cavity size or dimensions, therefore allowing for the most favorable orientations with the larger **Tol** guest molecule and not the smaller-sized **Py** to form stable host–guest intermolecular interactions.[21,29]

To further show the selectivity of **DIHO-cage** for **Tol**, we grew a single crystal in a 1:1 (v/v) mixture of toluene and pyridine. The orange single crystal obtained was analyzed using SCXRD and showed the same space group as that for the crystal obtained directly from toluene alone. This result confirmed the ability of **DIHO-cage** to selectively capture **Tol** from a **Tol/Py** mixture, a feature that can also be visualized due to the different colours of the crystals with/without **Tol** (Fig. 4 and Fig. S16–S18 and Table S1, ESI†). We then confirmed that the guest-free **DIHO-cage** can be regenerated from **DIHO-cage@Tol** simply by washing **DIHO-cage@Tol** with hexane and allowing it to dry at a very reduced temperature of 45 °C under vacuum. This approach ensured the robustness of the **DIHO-cage**, allowing it to withstand several adsorption–desorption processes/cycles while retaining its performance (Fig. S19 and 20, ESI†).

To further establish and corroborate the affinity of the **DIHO-cage** for **Tol**, a gas chromatography (GC) analysis was carried out. The results confirmed the adsorption and selectivity of **Tol** over **Py** by **DIHO-cage** with 99.5% purity (Fig. 5a and b) in one adsorption cycle. This high 99.5% purity of captured **Tol** persisted through five cycles of adsorption, and the purity of the **Py** left behind improved to *ca.* 100% (Fig. 5c and Fig. S21, ESI†). This observation further confirmed that obtaining highly pure **Py** could also be achieved.

In summary, we have successfully demonstrated that a polar crystalline organic cage (**DIHO-cage**) can selectively adsorb only toluene in 1:1, 1:3 and 3:1 (v/v) **Tol/Py** binary mixtures. **DIHO-cage** was found in this work to show a pair of advantages: efficient **Tol** uptake (99.5%) and subsequent superior purification of pyridine after a few cycles of adsorption. Despite **DIHO-cage** having the hydrogen donor hydroxyl group (–OH), it could only act as a hydrogen bond acceptor to form a host–guest
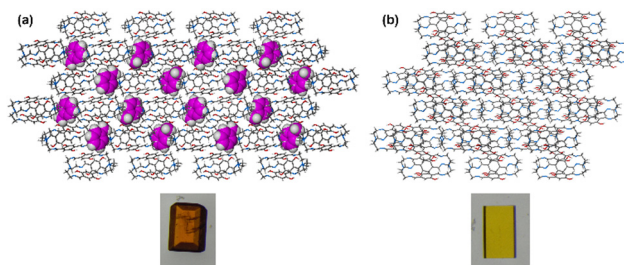

Fig. 3 Crystal packing showing various host–guest intermolecular interactions in **DIHO-cage@Tol**.

Fig. 4 Crystal packing and images of (a) **DIHO-cage@Tol** and (b) empty **DIHO-cage@Py** showing the vapochromic behaviour of **DIHO-cage**.

Fig. 5 (a) Relative amounts of **Tol** and **Py** adsorbed by activated DIHO-cage. (b) Percentages of **Tol** and **Py** adsorbed by activated DIHO-cage as determined using GC-MS. (c) Relative uptakes of **Tol** and **Py** after each of 5 adsorption processes/cycles.

complex with toluene (H-bond donor) instead of pyridine (H-bond acceptor) *via* numerous host/guest C–H···O and C–H···π intermolecular interactions as revealed by their crystal structures. This interesting phenomenon endows **DIHO-cage** with an ability not displayed by some recently reported adsorptive materials, namely to capture only toluene from a Tol/Py azeotrope mixture. This selective uptake and subsequent purification are accompanied with a color change, enabling the direct visualization of the entire adsorption of **Tol** by **DIHO-cage**. We believe that this result would serve as an excellent precedent for more remarkable separations of other azeotrope mixtures using organic cages.

All authors have given approval to the final version of the manuscript.

Data availability

The data supporting this article have been included as part of the ESI† with the crystallographic data for all the structures deposited at the CCDC and accessible at https://www.ccdc.cam.ac.uk/structures.

Conflicts of interest

There are no conflicts to declare.

Notes and references

1 G. Modla, *Energy*, 2013, **50**, 103–109.

2 Pyridine Market Size by Type. Regions, Global Industry Analysis, Share, Growth, Trends, and Forecast 2024 to 2033, https://www.thebrainyinsights.com/report/pyridine-market-14125.
3 C. H. Schneider and C. C. Lynch, *J. Am. Chem. Soc.*, 1943, **65**, 1063.
4 D. R. Lide, *CRC Handbook of Chemistry and Physics*, CRC Press, Boca Raton, FL, 2005, pp. 6–194. Internet version: https://www.hbcpnetbase.com, accessed 2021-10-30.
5 M. Errico, B.-G. Rong, G. Tola and M. Spano, *Ind. Eng. Chem. Res.*, 2013, **52**, 1612–1619.
6 W. L. Luyben, *Chem. Eng. Process.*, 2018, **123**, 174–184.
7 S. Liang, Y. Cao, X. Liu, X. Li, Y. Zhao, Y. Wang and Y. Wang, *Chem. Eng. Res. Des.*, 2017, **117**, 318–335.
8 Y. Wang, X. Zhang, X. Liu, W. Bai, Z. Zhu, Y. Wang and J. Gao, *Sep. Purif. Technol.*, 2018, **191**, 8–26.
9 J. Qi, Y. Li, J. Xue, R. Qiao, Z. Zhang and Q. Li, *Sep. Purif. Technol.*, 2020, **238**, 116487.
10 J. R. Wu and Y. W. Yang, *Angew. Chem., Int. Ed.*, 2021, **60**, 1690–1701.
11 K. C. Jie, Y. J. Zhou, E. R. Li and F. Huang, *Acc. Chem. Res.*, 2018, **51**, 2064–2072.
12 A. Dey, S. Chand, B. Maity, P. M. Bhatt, M. Ghosh, L. Cavallo, M. Eddaoudi and N. M. Khashab, *J. Am. Chem. Soc.*, 2021, **143**, 4090–4094.
13 H. Yao, Y. M. Wang, M. Quan, M. U. Farooq, L. P. Yang and W. Jiang, *Angew. Chem., Int. Ed.*, 2020, **59**, 19945–19950.
14 A. Dey, S. Chand, M. Ghosh, M. Altamimy, B. Maity, P. M. Bhatt, I. A. Bhat, L. Cavallo, M. Eddaoudi and N. M. Khashab, *Chem. Commun.*, 2021, **57**, 9124–9127.
15 B. Hua, Y. Ding, L. O. Alimi, B. Moosa, G. Zhang, W. S. Baslyman, J. Sessler and N. M. Khashab, *Chem. Sci.*, 2021, **12**, 12286–12291.
16 X. Liu, L. O. Alimi and N. M. Khashab, *Chem. Commun.*, 2022, **58**, 9369–9372.
17 B. Moosa, L. O. Alimi, W. Lin, A. Fakim, P. M. Bhatt, M. Eddaoudi and N. M. Khashab, *Angew. Chem., Int. Ed.*, 2023, **62**, e202311555.
18 D. Luo, J. Tian, J. L. Sessler and X. Chi, *J. Am. Chem. Soc.*, 2021, **143**, 18849–18853.
19 Q. Li, K. Jie and F. Huang, *Angew. Chem., Int. Ed.*, 2020, **59**, 5355–5358.
20 (a) M. Liu, R. Cen, J. Li, Q. Li, Z. Tao, X. Xiao and L. Isaacs, *Angew. Chem., Int. Ed.*, 2022, **61**, e202207209; (b) B. Li, Y. Wang, Y. Wang, Y. Liu, L. Wang, Z.-Y. Zhang and C. Li, *Chem. Commun.*, 2024, **60**, 6889–6892; (c) B. Hua, L. Shao, M. Li, H. Liang and F. Huang, *Acc. Chem. Res.*, 2022, **55**, 1025–1034; (d) J.-R. Wu, Z. Cai, G. Wu, D. Dai, Y.-Q. Liu and Y.-W. Yang, *J. Am. Chem. Soc.*, 2021, **143**, 20395–20402.
21 L. O. Alimi, B. Moosa, W. Lin and N. M. Khashab, *ACS Mater. Lett.*, 2024, **6**, 1467–1473.
22 Z. Cai, J. Du, T. Huang, Y. Ding and M. Wu, *CrystEngComm*, 2023, **25**, 5778–5781.
23 S. La Cognata and V. Amendola, *Chem. Commun.*, 2023, **59**, 13668–13678.
24 T. Tozawa, J. T. A. Jones, S. I. Swamy, S. Jiang, D. J. Adams, S. Shakespeare, R. Clowes, D. Bradshaw, T. Hasell, S. Y. Chong, C. Tang, S. Thompson, J. Parker, A. Trewin, J. Bacsa, A. M. Z. Slawin, A. Steiner and I. A. Cooper, *Nat. Mater.*, 2009, **8**, 973–978.
25 B. Moosa, L. O. Alimi, A. Shkurenko, A. Fakim, P. M. Bhatt, G. Zhang, M. Eddaoudi and N. M. Khashab, *Angew. Chem., Int. Ed.*, 2020, **59**, 21367–21371.
26 Y. Ding, L. O. Alimi, B. Moosa, C. Maaliki, J. Jacquemin, F. Huang and N. M. Khashab, *Chem. Sci.*, 2021, **12**, 5315–5318.
27 L. O. Alimi, F. Fang, B. Moosa, Y. Ding and N. M. Khashab, *Angew. Chem., Int. Ed.*, 2022, **61**, e202212596 (*Angew. Chem.*, 2022, **134**, e202212596).
28 A. C. Eaby, D. C. Myburgh, A. Kosimov, M. Kwit, C. Esterhuysen, A. M. Janiak and L. J. Barbour, *Nature*, 2023, **616**, 288–292.
29 K. J. Hartlieb, J. M. Holcroft, P. Z. Moghadam, N. A. Vermeulen, M. M. Algaradh, M. S. Nassar, Y. Y. Botros, R. Q. Snurr and J. F. Stoddart, *J. Am. Chem. Soc.*, 2016, **138**, 2292–2301.